

Sparsely-Spread CDMA - a statistical mechanics based analysis

Jack Raymond and David Saad

Neural Computation Research Group, Aston University, Aston Triangle, Birmingham,
B4 7EJ

E-mail: jack.raymond@physics.org

Abstract.

Sparse Code Division Multiple Access (CDMA), a variation on the standard CDMA method in which the spreading (signature) matrix contains only a relatively small number of non-zero elements, is presented and analysed using methods of statistical physics. The analysis provides results on the performance of maximum likelihood decoding for sparse spreading codes in the large system limit. We present new results for both cases of regular and irregular spreading matrices, with a comparison to the canonical (dense) random spreading code.

PACS numbers: 64.60.Cn, 75.10.Nr, 84.40.Ua, 89.70.+c

AMS classification scheme numbers: 68P30,82B44,94A12,94A14

1. Background

The subject of multiuser communications is one of great interest from both theoretical and engineering perspectives [1]. Code Division Multiple Access (CDMA) is a particular method for allowing multiple users to access channel resources in an efficient and robust manner, and plays an important role in the current preferred standards for allocating channel resources in wireless communications. CDMA utilises channel resources highly efficiently by allowing many users to transmit on much of the bandwidth simultaneously, each transmission being encoded with a user specific signature code. Disentangling the information in the channel is possible by using the properties of these codes and much of the focus in CDMA is on developing efficient codes and decoding methods.

In this paper we study a variant of the original method, sparse CDMA, where the spreading matrix contains only a relatively small number of non-zero elements. While the straightforward application of sparse CDMA techniques to uplink multiple access communication is rather limited, as it is difficult to synchronise the sparse transmissions from the various users, the method can be highly useful for frequency and time hopping. In frequency-hopping code division multiple access (FH-CDMA), one repeatedly switches frequencies during radio transmission, often to minimize the effectiveness of interception or jamming of telecommunications. At any given time step, each user occupies a small (finite) number, G , of the (infinite) M -ary frequency-shift-keying (MFSK) of gain G (the total number of chip-frequency pairs is therefore MG .) Hops between available frequencies can be either random or preplanned and take place after the transmission of data on a narrow frequency band. In time-hopping (TH-)CDMA, a pseudo-noise sequence defines the transmission moment for the various users, which can be viewed as sparse CDMA when used in an ultra-wideband impulse communication system. In this case the sparse time-hopping sequences reduces collisions between transmissions.

Recently it has been noted that certain types of structurally disordered codes, in particular low-density codes, may have particularly valuable features and are also particularly suitable for analysis by methods developed within the framework of statistical mechanics of disordered systems [2, 3]. For the purposes of the current analysis the replica method is used, a powerful method known to give exact results for many systems. Supplementary analysis and interpretation are presented from a statistical physics perspective.

This work follows the seminal paper of Tanaka [4], and more recent extensions [5], in utilising the replica analysis for a randomly spread CDMA code with discrete inputs, which established many of the properties of random densely-spread codes with respect to several different detectors including Maximum A Posteriori (MAP) and minimum mean square-error (MMSE). Sparsely-spread CDMA differs from the conventional CDMA, based on dense spreading sequences, in that any user only transmits to a small number of chips (by comparison to transmission on all chips in the case of dense CDMA).

The feasibility of sparse CDMA for transmitting information was recently demonstrated [6] and several results for the case of a Gaussian prior distribution of input

symbols have been established, using primarily a replica method based analysis. In a separate recent study, based on the belief propagation inference algorithm and a binary input prior distribution, sparse CDMA has also been considered as a route to proving results in the densely spread code [7]. In addition this study demonstrated the existence of a *waterfall* phenomenon comparable to the dense code for a subset of ensembles. The waterfall phenomenon is observed in decoding techniques, where there is a dynamical transition between two statistically distinct solutions as some parameter (in this case noise) is varied. Finally we note a number of pertinent studies concerning the effectiveness of belief propagation as a MAP decoding method [8, 9, 10], and in combining sparse encoding (LDPC) methods with CDMA [11].

The theoretical work regarding sparsely spread CDMA remained lacking in certain respects. As pointed out in [6], spreading codes with Poisson distributed number of non-zero elements, per chip and across users, are systematically failing in that each user has some probability of not contributing to any chips (transmitting no information). Even in the “partly regular” code [7] ensemble (where each user transmits on the same number of chips) owing to the poisson distribution in number of contribution per chip some chips have no contributers, consequently the bandwidth is not effectively utilised. We circumvent this problem by introducing constraints to prevent this, namely taking regular signature codes constrained such that both the number of users per chip and chips per user take fixed integer values. Using new tools from statistical mechanics we are able to cast greater light on the nature of the binary prior transmission process. Notably the nature of the decoding state space and relative performance of sparse ensembles versus dense ones across a range of noise levels; and importantly, the question of how the phase coexistence found by Tanaka [4] extends to sparse ensembles, especially close to the transition points determined for the dense ensemble. Phase coexistence is here meant in the same sense as the water-ice phase coexistence, where two stable solutions (decodings) coexist for some parameterisation.

Within this paper we demonstrate the superiority of regular sparsely spread CDMA code over densely spread codes in certain respects, for example, the anticipated bit error rate arising in decoding is improved in the high noise regime and the phase coexistence behaviour is less pervasive. Furthermore, to utilise belief propagation for such an ensemble is certain to be significantly faster and less computationally demanding [12], which has clear power-consumption implications. Other practical issues of implementation, the most basic being non-synchronisation and power control, require detailed study and may make fully harnessing these advantages more complex and application dependent.

The paper is organised as follows: In section 2 we will introduce the general framework and notation used, while the methodology used for the various codes will be presented in section 3. The main results for the various codes will be presented in section 4 followed by concluding remarks in section 5.

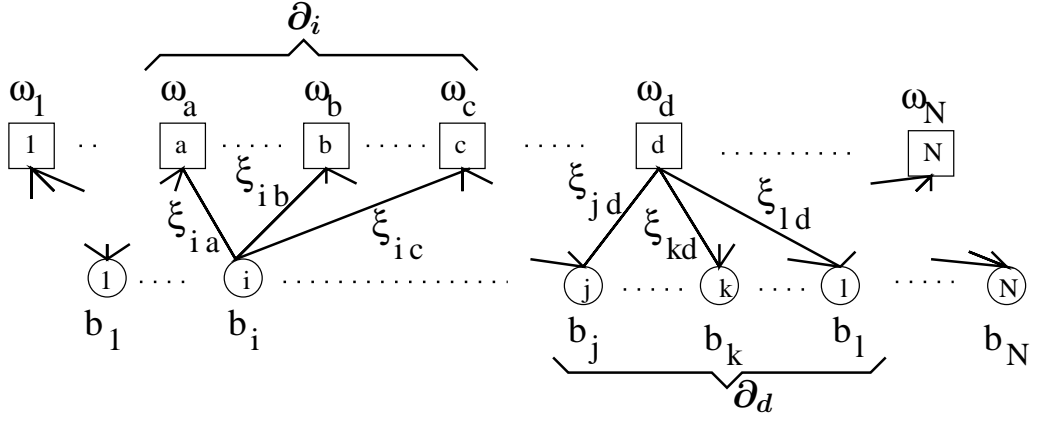


Figure 1. A bi-partite graph is useful for visually realising a problem. A user node i at the bottom interacts through its set of neighbouring factor nodes (∂i) to which it connects. The factor nodes are determined through a similar neighborhood. The interaction at each factor is conditioned on the input bits \mathbf{b} , the chip noise $\boldsymbol{\omega}$ and the modulation sequence ξ . The statistical mechanics reconstruction problem associates dynamical variables $\boldsymbol{\tau}$ to the user nodes that interact through the factors. As the system relaxes it in principle evolves to a state in which $\tau_i b_i \approx 1$ for each index i - in which $\boldsymbol{\tau}$ approximates \mathbf{b} , since each factor penalises deviation from this configuration (globally and approximately locally).

2. The model

We consider a standard model of CDMA consisting of K users transmitting in a bit interval of N chips. We assume a model with perfect power control and synchronisation, and consider only the single bit interval. In our case the received signal is described by

$$\mathbf{y} = \frac{1}{\sqrt{C}} \sum_{k=1}^K [\mathbf{s}_k b_k] + \boldsymbol{\omega} , \quad (1)$$

where the vector components describe the values for distinct chips: \mathbf{s}_k is the spreading code for user k , $b_k = \pm 1$ is the bit sent by user k , and $\boldsymbol{\omega}$ are the noise components. The spreading codes are sparse so that in expectation only C of the elements in vector \mathbf{s}_k are non-zero.

If, with knowledge of the signature matrix (\mathbf{s}) in use, we assume the signal has been subject to additive white Gaussian channel noise of variance σ^2 , we can write a probability distribution for the sent variables $\boldsymbol{\tau}$ (unknowns given the particular instance) as

$$P(\boldsymbol{\tau}, \mathbf{b}, \boldsymbol{\omega} | \mathbf{s}) = \prod_{\mu=1}^N \left[\frac{1}{\sqrt{2\pi\sigma^2}} \exp \left(\frac{1}{2\sigma^2} \left(\frac{1}{\sqrt{C}} \sum_{k=1}^K [s_{\mu k} (b_k - \tau_k)] + \omega_{\mu} \right)^2 \right) \right] , \quad (2)$$

and this may be manipulated by Bayes Theorem to give the likelihood for the inputs, mutual information, and other quantities. The statistical mechanics approach from here is to define a Hamiltonian and partition function from which the various statistics relating to this probability distribution may be determined - and hence all the usual information

theory measures. A suitable choice for the Hamiltonian is

$$\mathcal{H}(\boldsymbol{\tau}) = \sum_{\mu=1}^N \frac{1}{2\sigma^2} \left(\frac{1}{\sqrt{C}} \sum_{k=1}^K [s_{\mu k} (b_k - \tau_k)] + \omega_{\mu} \right)^2 + \sum_{k=1}^K h_k \tau_k . \quad (3)$$

We can here identify $\boldsymbol{\tau}$ as the dynamical variables in the reconstruction problem (dependence shown explicitly). The other quenched variables (parameters), describing the instance of the disorder, are the signature matrix (\mathbf{s}), noise ($\boldsymbol{\omega}$) and the inputs (\mathbf{b}). The variables h_k describe our prior beliefs about the inputs, but we assume that all inputs in the space $[+1, -1]^K$ are equi-probable, and so $h_k = 0$ from here onwards. The properties of such a system may be reflected in a factor (tanner) graph, a bipartite graph in which users and chips are represented by nodes (see figure 1).

The calculation we undertake is specific to the case of the thermodynamic limit in which the number of chips $N \rightarrow \infty$ whilst the load $\alpha = K/N$ is fixed. Note that α is termed β in many CDMA papers, here we reserve β to mean the “inverse temperature” in a statistical mechanics sense (which here defines different classes of optimal detectors or alternatively prior beliefs). Furthermore we consider two canonical forms of sparse signature matrix: regular and irregular (limited here to Poissonian constructions). In the regular code we have two parameters C and L , where C describes the number of non-zero elements in the spreading code of every user, and L the number of contributions to each chip. In the irregular ensemble we assume only an average number of non-zero chip contributions per user, \tilde{C} , with each user having an independently sampled code. Aside from these constraints all instances are equally likely. Finally notice that C and L define α (the spreading ratio) through the relation,

$$\alpha = \frac{K}{N} = \frac{L}{C} . \quad (4)$$

The case in which α is greater than 1 will be called oversaturated, since more than one bit is being transmitted per chip.

3. Methodology

3.1. Regular Codes

We determine the properties of the above model through a statistical mechanics framework, using the replica method. From the expression of the Hamiltonian (3) we may identify a free energy and partition function as:

$$f = -\frac{1}{N\beta} \ln Z \quad Z = \text{Tr}_{\boldsymbol{\tau}} \exp(-\beta \mathcal{H}(\boldsymbol{\tau})) .$$

To progress we make use of the anticipated *self-averaging* properties of the system. The assumption being that in the large system limit any two randomly selected instances will, with high probability, have indistinguishable statistical properties. This assumption has firm foundation in several related problems [13], and is furthermore intuitive after some reflection. If this assumption is true then the statistics of any particular instance

can be described completely by the free energy averaged over all instances of the disorder. We are thus interested in the quantity

$$\mathcal{F} = \langle f \rangle = - \lim_{N \rightarrow \infty} \frac{1}{N\beta} \langle \ln Z \rangle_I , \quad (5)$$

where the angled brackets represented the weighted averages over I (the instances). Taking the average over disorder is a difficult problem which is why we make use of the replica identity

$$\langle \ln Z \rangle_I = \lim_{n \rightarrow 0} \frac{\langle Z^n \rangle_I - 1}{n} . \quad (6)$$

We can model the system now as one of interacting replicas, where Z^n is decomposed as a product of an integer number of partition functions with conditionally independent (given the instance of the disorder) dynamical variables. The discreteness of replicas is essential in the first part of the calculation, but a continuation to the real numbers is required in taking $n \rightarrow 0$ – this is a notorious assumption and which rigorous mathematics can not yet justify. However, we shall assume validity and since the methodology for the sparse structures is well established [14, 13] we omit our particular details.

The concise form for our equations is attained using the assumption of replica symmetry (RS). This amounts to the assumption that the correlations amongst replica are all identical, and determined by a unique shared distribution. The validity of this assumption may be self consistently tested (section 3.3). Using Laplace's method, this gives the following expression for the (RS) free energy

$$\mathcal{F}_{RS} = - \frac{1}{\beta} \text{Extr}_{\pi, \hat{\pi}} (\mathcal{G}_{1,RS} + \mathcal{G}_{2,RS} + \mathcal{G}_{3,RS}) \quad (7)$$

where

$$\mathcal{G}_{1,RS} = -L \ln 2 + \int \prod_{l=1}^L [\text{d}\pi(x_l)] \langle \ln \text{Tr}_{\{s_l=\pm 1\}} \chi_L(\mathbf{s}; \{\xi\}, \omega) \rangle_{\omega, \{\xi\}} ; \quad (8a)$$

$$\chi_L(\mathbf{s}; \{\xi\}, \omega) = \exp \left(-\frac{\beta}{2\sigma^2} \left(\omega + \frac{1}{\sqrt{C}} \sum_{l=1}^L (1 - s_l) \xi_l \right)^2 \right) \prod_{l=1}^L (1 + s_l x_l) ; \quad (8b)$$

$$\mathcal{G}_{2,RS} = -L \int \text{d}\pi(u) \text{d}\hat{\pi}(h) \ln(1 + uh) ; \quad (8c)$$

$$\mathcal{G}_{3,RS} = \alpha \int \prod_{c=1}^C [\text{d}\hat{\pi}(h_c)] \ln \left(\prod_{c=1}^C (1 + h_c) + \prod_{c=1}^C (1 - h_c) \right) . \quad (8d)$$

The averages are taken with respect to the true noise distribution ω , and L identical distributions for ξ . Note that we have used the convention of magnetisations rather than fields – this is the form used in numerical investigation where it proved more stable (section 4).

In attaining these expressions we have made the following assumptions, aside from the inherent assumptions of the replica method. (1) The variables $\xi_{\mu,k}$ are drawn independently and at random from a single (symmetric) distribution. (2) Instances of the noise ω_μ are

drawn independently from a single distribution. (3) All signature matrices meeting the regularity criteria are equally likely. Furthermore, in order to defend the self-averaging assumption, it is necessary that the distributions for ξ and ω have finite moments. The calculation can also be done for a non-symmetric distribution of $\xi_{\mu,k}$, in particular $\xi_{\mu,k} = 1$ is interesting, but the resulting equations are slightly more involved since one cannot gauge \mathbf{b} to the distribution on ξ in this case. This gauging explains the ability to take an exact average for b in the expressions (8a-8d).

As the free energy is minimised at equilibrium, the order parameter distributions $\{\pi, \hat{\pi}\}$ are chosen so as to extremise (7). The self consistent equations attained by the saddle point method are:

$$\hat{\pi}(\hat{x}) = \int \prod_{l=1}^{L-1} [d\pi(x_l)] \left\langle \delta \left(\hat{x} - \frac{\text{Tr}_{\{s_l=\pm 1\}} s_L \bar{\chi}_L(\mathbf{s}; \{\xi\}, \omega)}{\text{Tr}_{\{s_l=\pm 1\}} \bar{\chi}_L(\mathbf{s}; \{\xi\}, \omega)} \right) \right\rangle_{\{\xi\}, \omega} \quad (9a)$$

$$\bar{\chi}_L(\mathbf{s}; \{\xi\}, \omega) = \exp \left(-\frac{\beta}{2\sigma^2} \left(\omega + \frac{1}{\sqrt{C}} \sum_{l=1}^L (1 - s_l) \xi_l \right)^2 \right) \prod_{l=1}^{L-1} (1 + s_l x_l) \quad (9b)$$

$$\pi(x) = \int \prod_{c=1}^{C-1} [d\hat{\pi}(\hat{x}_c)] \delta \left(x - \frac{\prod_{c=1}^{C-1} (1 + \hat{x}_c) - \prod_{c=1}^{C-1} (1 - \hat{x}_c)}{\prod_{c=1}^{C-1} (1 + \hat{x}_c) + \prod_{c=1}^{C-1} (1 - \hat{x}_c)} \right). \quad (9c)$$

The equations as presented may be solved by population dynamics [15], a method in which one makes a histogram approximation to the functions $\{\pi, \hat{\pi}\}$ and iterates these until some convergence criteria is met.

The other quantities of interest may be determined from the probability distribution for the overlap of reconstructed and sent variables $m_k = \langle b_k \tau_k \rangle$,

$$P(m) = \frac{1}{K} \sum_{k=1}^K \delta_{m_k, m} \propto \int \prod_{c=1}^C [d\hat{\pi}(\hat{x}_c)] \delta \left(h - \frac{\prod_{c=1}^C (1 + \hat{x}_c) - \prod_{c=1}^C (1 - \hat{x}_c)}{\prod_{c=1}^C (1 + \hat{x}_c) + \prod_{c=1}^C (1 - \hat{x}_c)} \right), \quad (10)$$

and the entropy density may be calculated from the free energy density by use of the relation

$$s = \beta(e - f), \quad (11)$$

where e is the energy.

3.2. Irregular Codes

Here we summarise the differences in method and results attained for the irregular ensemble in which each element is non-zero independently with probability \tilde{C} , and only total energy received over the chip interval (not per chip or per user) is controlled. The expressions found are comparable, but with C and L now drawn from Poissonian distributions parameterised by \tilde{C} and α . This is manifested in (8a-8d) as

$$\mathcal{G}_{1,RS} = -\tilde{L} \ln 2 + \left\langle \int \prod_{l=1}^L d\pi(x_l) \langle \ln \text{Tr}_{\{s_l=\pm 1\}} \chi_L(\mathbf{s}; \{\xi\}, \omega) \rangle_{\omega, \{\xi\}} \right\rangle_L; \quad (12a)$$

$$\mathcal{G}_{2,RS} = -\tilde{L} \int d\pi(x) \int \hat{\pi}(\hat{x}) \ln(1 + x\hat{x}) ; \quad (12b)$$

$$\mathcal{G}_{3,RS} = \alpha \left\langle \int \prod_{c=1}^C d\hat{\pi}(\hat{x}_c) \ln \left(\prod_{c=1}^C (1 + \hat{x}_c) + \prod_{c=1}^C (1 - \hat{x}_c) \right) \right\rangle_C . \quad (12c)$$

where C is drawn from a distribution of mean \tilde{C} , and L from one with a mean of $\tilde{L} = \tilde{C}\alpha$. From equations (12a-12c), the other statistics are attained with analogous modifications to the regular case.

3.3. Stability Analysis

To test the stability of the obtained solutions we consider both the appearance of non-negative entropy, and a stability parameter defined through a consideration of the fluctuation dissipation theorem. The first criteria that the entropy be non-negative is based on the fact that physically viable solutions in discrete systems must have positive entropy so that any solution found not meeting this criteria must be based on bad premises; replica symmetry breaking is typically the likely source.

The stability parameter λ is defined in connection with the cavity method for spin glasses [16]. If one considers a particular instance of the problem, such as would be described by the factor graph figure 1, then one can develop a set of equations describing the local magnetic fields. The method will not be presented here, but one can establish by the cavity method a set of equations identical to those in (9a-9c), and also found elsewhere in the form of belief propagation equations. Messages passed between factor (a) and user (i) nodes give rise to self consistent equations:

$$x_{i \rightarrow a} = \frac{1}{\mathcal{N}_x} \prod_{c \in \partial i \setminus a} (1 + \hat{x}_c) - \prod_{c \in \partial i \setminus a} (1 - \hat{x}_c) ; \quad (13a)$$

$$\begin{aligned} \hat{x}_{a \rightarrow i} = & \left\langle \frac{1}{\mathcal{N}_{\hat{x}}} \text{Tr}_{\{s_l = \pm 1\}} s_L \exp \left(-\frac{\beta}{2\sigma^2} \left(\omega + \frac{1}{\sqrt{C}} \sum_{l \in \partial a \setminus i}^L (1 - s_l) \xi_l \right)^2 \right) \right. \\ & \left. \times \prod_{l \in \partial a \setminus i} (1 + s_l x_{l \rightarrow a}) \right\rangle_{\{\xi\}, \omega} ; \end{aligned} \quad (13b)$$

where $\mathcal{N}_{x, \hat{x}}$ are the relevant normalisations, and the abbreviation ∂y indicates the set of nodes connected to y .

One can then define chains of variables connected through factor nodes. If we consider a path of length d , defined by a sequence links ($i \rightarrow a, a \rightarrow j$), between two distant nodes we can define the susceptibility of τ_d , the final node, to a change in τ_0 , the root node. If we assume the paths are long, effectively independent and self-averaging then we can determine the connected correlation function between the two users as

$$\lambda = \lim_{d \rightarrow \infty} C \alpha^d \prod_{i \rightarrow j} \frac{\partial x_{i \rightarrow a}}{\partial \hat{x}_{b \rightarrow i}} \frac{\partial \hat{x}_{b \rightarrow i}}{\partial x_{j \rightarrow b}} , \quad (14)$$

where C is a constant of order one, and α^d is the number of users at distance d in the graph. It turns out that these assumptions may be self consistently applied to the

sparsely connected ensemble. The relation between RS and the connected correlation function is that for RS to be valid the connected correlation must decrease asymptotically (exponentially) with distance d . Therefore we calculate $1/d \ln \lambda$ and determining if this is greater than 0 in order to test for instabilities due to RS. This can be done simultaneously with the population dynamics [17].

3.4. Information Capacity Upper Bound

Finally, note that in several places the inferiority of the irregular ensembles (partly regular and fully Poissonian) is suggested based on the knowledge that codes which leave a portion of the bandwidth unutilised cannot be optimal. Though we do not prove this, there is an obvious upper bound to the load the channel can bear with discrete inputs and still achieve capacity that gives some indication as to why and by how much this discrepancy exists. Also this is a useful upper bound which places a restriction on the load α which can be supported for a particular density (defined by L or \tilde{L}), and we present cases not exceeding this bound.

The free energy is upper bounded by assuming a factorised form for the partition sum, separating it into single chip components,

$$\mathcal{F} = - \lim_{N \rightarrow \infty} \frac{1}{N\beta} \langle \ln Z \rangle_I > - \lim_{N \rightarrow \infty} \frac{1}{N\beta} \langle \ln \prod_{\mu} Z_{\mu}(\omega_{\mu}, \mathbf{s}_k) \rangle_I .$$

We can relate the free energy to the spectral efficiency and so upper bound the total amount of information a particular sparse code ensemble is capable of transmitting. Conveniently, the upper bound presented depends only on the noise distribution, the prior on the transmitted bits, and the distribution in number of inputs to each chip. We find the upper bound for the regular code is greater than the irregular ensembles, due to the differences in distributions for L – the irregular ensembles considered are characterised by a Poissonian number of contributions for each chip.

4. Results

Results are presented here for the canonical case of Binary Phase Shift Keying (BPSK), in which the non-zero elements of the spreading codes, $\xi_{k,\mu} = \pm 1$. Furthermore we assume a noise model for the true noise ω which is also AWGN, but with a noise level parameterised now by σ_0^2 . This allows us to define a signal to noise ratio, $SNR = \alpha\sigma_0^{-2}$ (the corresponding power spectral density, against which statistics are plotted is half this value). For evaluation purposes we assume the channel noise level is known precisely, so that $\sigma_0 = \sigma$, and employ the Nishimori temperature [2] ($\beta = 1$). This also guarantees that the RS solution is thermodynamically dominant. Where of interest we plot the comparable statistics for the single user Gaussian channel (SUG), and the densely spread ensemble, each with IO (individually optimum) decoders – equivalent to maximum likelihood for individual bits.

Study of this system is primarily constrained by the nature of equations (9a-9c). No exact solutions are apparent, and perturbative regimes about the ferromagnetic solution (which is only a solution for zero noise) are difficult to handle. Consequently we use population dynamics [15] – representing the distribution of fields $\{\pi(x), \hat{\pi}(\hat{x})\}$ by finite populations (histograms) and iterating this distribution until convergence. In each field update $\{x_i, \hat{x}_i\}$, we consider only a single random sample for each integral, or average, in (9a-9c), and update the entire population ($\{x_i\}$ or $\{\hat{x}_i\}$) sequentially. It is hoped, and observed, that the large number of fields sampled in this way converges towards the true distribution to leading order in N , the number of fields in the population. Computer resources however restrict the cases studied in detail to an intermediate noise spectral density regime, and small \tilde{L}, L . In particular, the problem at high noise levels, is the Gaussian noise average, which is poorly estimated, while at low noise a majority of the histogram is concentrated at magnetisations $x, \hat{x} \approx 1$ not allowing sufficient resolution in the rest of the histogram.

Two parallel populations are initialised either uniformly at random, or in the ferromagnetic state. These two populations are known to converge towards the unique solution, where one exists, from opposite directions, and so we can use their convergence as a criteria for halting the algorithm and testing for the appearance of multiple solutions. In the case where they converge to different solutions we can identify the solution converged to from the ferromagnetic state as a *good* solution - in the sense that it reconstructs well, and that arrived at from random conditions as a *bad* solution. In the equivalent BP propagation we cannot choose initial conditions equivalent to ferromagnetic – knowing the exact solution would of course makes the decoding redundant. We therefore expect the properties of the *bad* solution to be those realisable by belief propagation (though clever algorithms may be able to escape to the good solution under some circumstances).

In order to approximate the stability parameter λ one can attach a stability measure $\{\nu_i, \hat{\nu}_i\}$ to each of the fields and calculate the average susceptibility, weighted by these values, simultaneously as each field is updated. In so doing we calculate the net correlation at a distance (d iterations) from the initial fields. Two values of $1/d \ln \lambda$ can then be determined by the relative decrease in $\sum \nu_i$ or $\sum \hat{\nu}_i$ in successive updates of the histograms. Whenever the field distributions converge, and sufficient resolution could be attained, this parameter strongly indicates the suitability of RS – including those regimes with multiple RS solutions (phase coexistence).

Several different measures are calculated from the converged order parameter, indicating the performance of sparse CDMA. Using the converged histograms for the fields we are able to determine the quantities free energy, energy and a histogram for the probability distribution, from discretisations of the previously presented equations (9a-9c). Using the probability distribution we are also able to approximate the decoding bit error rate

$$P_b = \int dP(x) \frac{1 - \text{sign}(x)}{2}; \quad (15)$$

multi-user efficiency

$$MuE = \frac{1}{SNR} [\operatorname{erfc}^{-1}(P_b)]^2 ; \quad (16)$$

and mutual information, $\alpha I(\mathbf{b}; \boldsymbol{\tau})$. The spectral efficiency is the capacity $I(\mathbf{b}; \mathbf{y})$ multiplied by the load, which is affine to the free energy (equivalently the entropy gap)

$$\nu = \alpha - s/\ln 2 . \quad (17)$$

We present our free energy measures in this form, since the ground state energy is attained in all systems (1/2), and the spectral efficiency in bits contains all the relevant information. Negative entropy can be identified when the measured spectral efficiency exceeds the load.

Figure 2 demonstrates some general properties of the regular ensemble in which C:L = 3:3. Equations (9a-9c) were iterated using population dynamics and the relevant properties were calculated using the obtained solutions; the data presented is averaged over 100 runs and error-bars are omitted for brevity. Figure 2(a) shows the bit error rate in regular and Poissonian codes. Regular codes show superior performance with respect to the dense case at high noise levels and are lower-bounded by the SUG performance. Poissonian codes show weaker performance in general, and at low noise levels in particular. A similar trend can be seen in figure 2(b) that shows the multiuser efficiency; where the performance of regular codes remains close to optimal for large SNR . Figure 2(c) shows the spectral efficiency and mutual information (solid and dot-dashed lines respectively for the various cases (which relate to the information loss); also here the performance of the sparse regular codes is similar to that of the dense case while the performance of Poissonian constructions is generally inferior. It was found in this case and all cases with unique solutions for given noise, that the algorithm converged to positive entropy values and to a stability measure $1/d \ln \lambda$ fluctuating about a value less than 0, as shown in figure 2(d). These points would indicate the suitability of the RS assumption.

Figure 3 indicates the effect of increasing density. As density is increased the performance of the sparse regular codes approaches that of the dense channel in terms of bit error rate (equivalently Multi-user efficiency in (a)) and spectral efficiency (b). We observed similar trends for the irregular cases, which rapidly approaches the performance of the regular case. However, for the irregular ensemble performance increases monotonically with density at all SNR . The rapid convergence to the dense case performance was elsewhere observed for partly regular ensembles, and ensembles based on a Gaussian prior input [6, 7]. To our knowledge the outperformance of the dense case by the sparse ensemble in terms of bit error rate is new, although by analogy with Time and Frequency Hopping codes this could be expected. At all densities the RS assumption was found to be valid where precision was available in the stability parameter.

Figure 4 indicates the effect of channel load α on performance. For small values of the load a monotonic increase in the bit error rate, and capacity are observed as L is increased, as shown in figures 4(a) and 4(b), respectively. The equivalent properties in the dense limit are also plotted. In the dense limit and $\alpha > 1.49$ there exist $SNRs$ for which 2 stable RS solutions exists [4], which can be seen in the multivalued nature of the

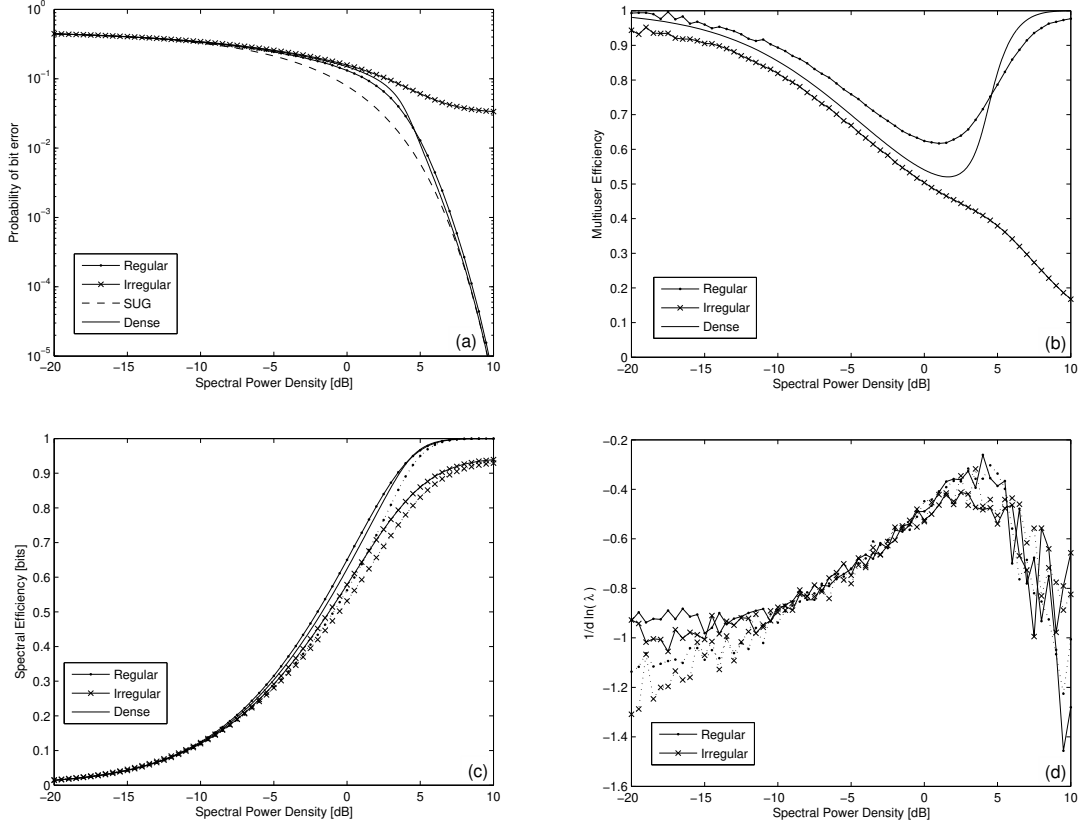


Figure 2. Performance of the sparse CDMA configuration $C = 3, L = 3$; all data presented on the basis of 100 runs, error bars are omitted and are typically small in subfigures (a)-(c) the smoothness of the curves being characteristic of this level, sufficient numerical accuracy could only be attained at intermediate $SNRs$. (a) The bit error rate is limited by the disconnected component in the case of irregular codes, regular codes are superior to the dense codes at high noise and lower-bounded by the SUG performance. (b) Multiuser efficiency indicates the performance of regular codes remains close to optimal for large SNR . (c) The spectral efficiency [——] and mutual information [· · · ·] indicate the information loss in the Maximum Likelihood decoding process, similar trends to the bit error rate and positive entropy. (d) The stability parameter suggests RS is suitable, the two lines represent two partially independent measures of the stability parameter in the converged systems, results are poor at high noise and low noise due to limitations in numerical accuracy.

curves for $\alpha = 5/3$ and $\alpha = 6/3$. For the irregular ensemble we found that for a density $\tilde{L} = 3$, there was evidence that only one solution persisted even with α as large as 2 (curves not plotted). For the regular ensemble the single state appeared to exist for the 5 : 3 ensemble, but at 6 : 3 we found evidence of a bimodal solution distribution, as shown in figures 4(a,b,c).

In the case of the 6 : 3 code we identified the onset of the bimodal distribution by noticing a divergence in the convergence time (the time for the ferromagnetic and random histograms to converge to a common distribution). The time for this to occur, in

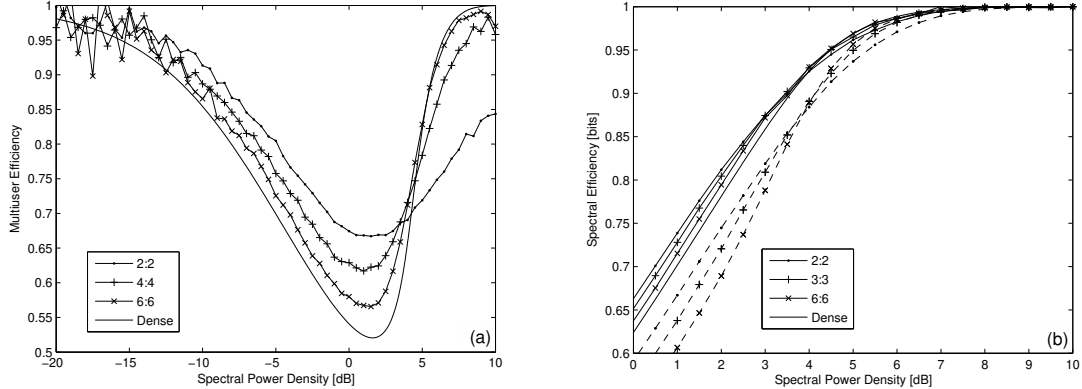


Figure 3. The effect of increasing density for the regular ensembles: (a) Multiuser efficiency and (b) spectral efficiency [——] with mutual information [---] vs. spectral power density. Data presented on the basis of 10 runs, error bars are omitted but of a size comparable with the smoothness of the curves. MuE is used to highlight the contrast (representing equivalent trends to P_b). For regular codes there exists some noise threshold above which lower density codes are preferable.

a heuristically chosen statistic and accuracy, is plotted in figure 4(d). By a naive linear regression across 3 decades we found a power law exponent of 0.59 and a transition point of $SNR = 21.11$, but cannot provide a goodness of fit measure to this data. This would represent the point at which at least two stable solutions co-exist (phase coexistence).

In figures 4(a,b) we indicate with a vertical line this transition point and show the statistical properties beyond this point. As can be seen in these subfigures they again adhere well to the dense case behaviour. Before the transition point (and beyond about 12 dB) the good and bad solutions coincide, indicating a narrow window in which the two solutions are bistable in a dynamical sense. If we interpret 4(b) in terms of free energy we see an apparent critical transition from the bad to good solution not far beyond the coexistence point. This cross-over corresponds to a point beyond which the bad solution has negative entropy –however our numerical work indicated that such a cross over was more often than not attributable to an insufficient convergence criteria, which we could not easily correct for in the high noise regime. Hence we cannot make strong conclusions about the existence and placement of this point. The stability parameters found beyond the transition point for both solution types are again negative in mean, but the measure is poorly resolved for the ‘good’ solution (figure 4(c)) in the coexistence regime, and for both solutions at lower noise.

The fact that these two solutions appear statistically well defined, and have negative stability parameters, does indicate that the RS assumption is probably correct (for $\beta = 1$) in a similar manner to the dense case in the phase coexistence region. Furthermore the phase coexistence behaviour found in the dense case appears to occur over a wider range of α and SNR values than in the sparse ensembles. Finally we observe that in the case presented, and others, it seems that the ‘bad’ solution of the sparse case always offers a

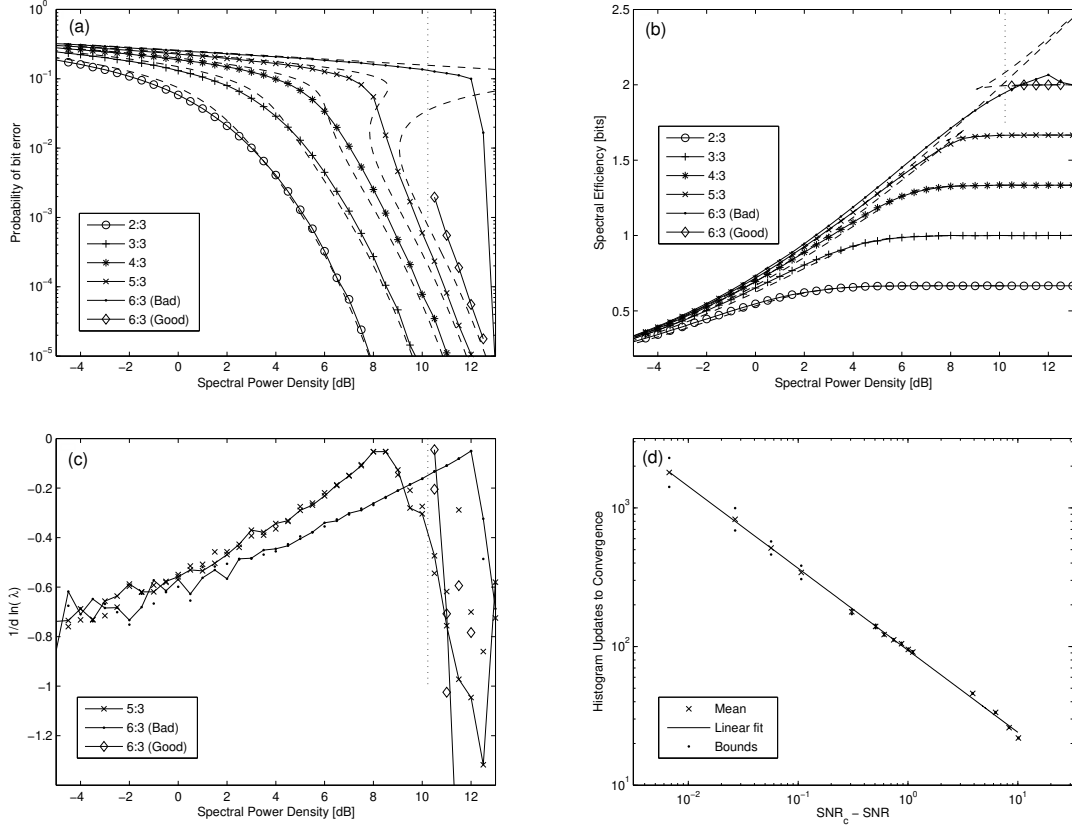


Figure 4. The effect of channel load α on performance for the regular ensemble. Data presented on the basis of 10 runs, error bars omitted but characterised by the smoothness of curves. Dashed lines indicate the dense code analogues. The vertical line indicates the point beyond which 6 : 3 good and bad solutions failed to converge to a single value, both dynamically stable solutions are shown beyond this point. (a) There is a monotonic increase in bit error rate with the load. (b) As load α is increased there is a monotonic increase in capacity. The spectral efficiency for the 'bad' solution exceeds 2 in a small interval (equivalent to negative entropy), but this is probably a manifestation of the inexact convergence or poor resolution of the histogram. (c) The Stability Parameter was found to be negative for all convergent solutions, indicating the suitability of RS. (d) Investigation of the the 6:3 code ($\alpha = 2$) indicates a divergence in convergence time as $SNR \rightarrow 21.107$ with exponent 0.59 based on a simple linear regression of 15 points (each point is the mean of 10 independent runs).

lower error-rate than the 'bad' case of the dense ensemble (and vice-versa for the good solutions). As such we can speculate that the transition point at which practical dense codes begin to outperform the sparse codes coincides with the dynamical transition point for the dense case.

Finally we present figure 5, which shows the limit in information capacity for the sparse code ensembles in the zero noise limit. This shows that at low densities the regular ensemble is clearly superior to the irregular ensembles for sufficiently low noise, while the gap closes as L or \tilde{L} increases.

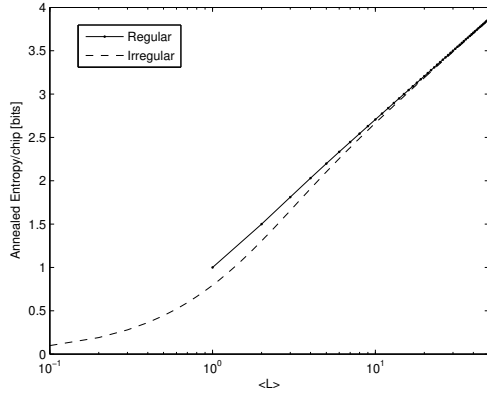


Figure 5. A zero noise limit annealed approximation to the capacity/chip of different codes. This upper bound to the capacity (maximum load) differs between fully regular and irregular ensembles, but becomes increasingly small as L or \tilde{L} increases.

5. Concluding Remarks

Our results demonstrate the feasibility of sparse regular codes for use in CDMA. At moderate noise levels it seems the performance of sparse regular codes may be very good. With the replica symmetric assumption apparently valid at practical SNR it is likely that fast algorithms based on belief propagation may be very successful in achieving the theoretical results. Furthermore for lower density sparse codes the problem of the bad solution, which limits the performance of practical decoding methods, seems to be less extensive in the over saturated regime.

Similarly a direct evaluation of the properties of belief propagation may prove similar results. In the absence of replica symmetry breaking states it is generally true that belief propagation performs very well. However, to make best use of the channel resources it may be preferable to implement high load regimes in the low noise cases, and so overcoming the algorithmic problems arising from the waterfall phenomenon is a challenge of practical interest in this case.

Other practical issues in implementation are certainly significant. Similar to the case of dense CDMA there are significant problems relating to multipath, fading and power control, in fact it is known that these effects are more disruptive for the sparse codes, especially regular codes. However, certain situations such as broadcasting (one to many) channels and downlink CDMA, where synchronisation can be assumed, may be practical points for future implementation. There are practical advantages of the sparse case over dense and orthogonal codes in some regimes.

The sparse CDMA method is likely to be particularly useful in frequency-hopping and time-hopping code division multiple access (FH and TH -CDMA) where the effect of these practical limitations is less emphasised.

Extensions based on our method to cases without power control or synchronisation have been attempted and are quite difficult. A consideration of priors on the inputs, in

particular the effects when sparse CDMA is combined with some encoding method may also be interesting.

Acknowledgments

Support from EVERGROW, IP No. 1935 in FP6 of the EU is gratefully acknowledged. DS would like to thank Ido Kanter for helpful discussions.

Bibliography

- [1] V. Sergio. *Multiuser Detection*. Cambridge University Press, New York, NY, USA, 1998.
- [2] H. Nishimori. *Statistical Physics of Spin Glasses and Information Processing*. Oxford Science Publications, 2001.
- [3] M. Mezard, G. Parisi, and M.A. Virasoro. *Spin Glass Theory and Beyond*. World Scientific, 1987.
- [4] Toshiyuki Tanaka. A statistical-mechanics approach to large-system analysis of cdma multiuser detectors. *Information Theory, IEEE Transactions on*, 48(11):2888–2910, 2002.
- [5] D. Guo and S. Verdu. *Communications, Information and Network Security*, chapter Multiuser Detection and Statistical Mechanics, pages 229–277. Kluwer Academic Publishers, 2002.
- [6] M. Yoshida and T. Tanaka. Analysis of sparsely-spread cdma via statistical mechanics. In *Proceedings - IEEE International Symposium on Information Theory, 2006.*, pages 2378–2382, 2006.
- [7] A. Montanari and D. Tse. Analysis of belief propagation for non-linear problems: The example of cdma (or: How to prove tanaka’s formula). In *Proceedings IEEE Workshop on Information Theory*, 2006.
- [8] Y. Kabashima. A cdma multiuser detection algorithm on the basis of belief propagation. *Jour. Phys. A*, 36(43):11111–11121, 2003.
- [9] J.P Neirotti and D. Saad. Improved message passing for inference in densely connected systems. *Europhys. Lett.*, 71(5):866–872, 2005.
- [10] A. Montanari, B. Prabhakar, and D. Tse. Belief propagation based multiuser detection. In *Proceedings of the Allerton Conference on Communication, Control and Computing, Monticello, USA*, 2006.
- [11] T. Tanaka and D. Saad. A statistical-mechanical analysis of coded cdma with regular ldpc codes. In *Proceedings - IEEE International Symposium on Information Theory, 2003.*, page 444, 2003.
- [12] D.J. MacKay. *Information Theory, Inference and Learning Algorithms*. Cambridge University Press, 2004.
- [13] R. Vicente, D. Saad, and Y. Kabashima. *Advances in Imaging and Electron Physics*, volume 125, chapter Low Density Parity Check Codes - A statistical Physics Perspective, pages 231–353. Academic Press, 2002.
- [14] K.Y.M. Wong and D. Sherrington. Graph bipartitioning and spin-glasses on a random network of fixed finite valence. *J. Phys. A*, 20:L793–99, 1987.
- [15] M. Mezard and G. Parisi. The bethe lattice spin glass revisited. *Euro. Phys. Jour. B*, 20(2):217–233, 2001.
- [16] O. Rivoire, G. Biroli, O.C. Martin, and M. Mzard. Glass models on bethe lattices. *Euro. Phys. J. B*, 37:55–78, 2004.
- [17] J. Raymond, A. Sportiello, and L. Zdeborova. The phase diagram of random 1-in-3 satisfiability problem. Preprint cond-mat/0702610, 2006.